

# Phonon dispersion of graphite

J. Maultzsch<sup>\*</sup>, S. Reich<sup>†</sup>, C. Thomsen<sup>\*</sup>, H. Requardt<sup>\*\*</sup> and P. Ordejón<sup>‡</sup>

<sup>\*</sup>*Institut für Festkörperphysik, Technische Universität Berlin, Hardenbergstr. 36, 10623 Berlin, Germany*

<sup>†</sup>*Department of Engineering, University of Cambridge, Cambridge CB2 1PZ, United Kingdom*

<sup>\*\*</sup>*European Synchrotron Radiation Facility (ESRF), B.P. 220, 38043 Grenoble, France*

<sup>‡</sup>*Institut de Ciència de Materials de Barcelona (CSIC), Campus de la Universitat Autònoma de Barcelona, 08193 Bellaterra, Barcelona, Spain*

**Abstract.** The phonon dispersion of graphite was determined by inelastic X-ray scattering along the  $\Gamma$ - $K$ ,  $K$ - $M$ , and  $\Gamma$ - $K$  direction. In contrast to many predictions, the dispersion of the transverse branch is large, leading to a minimum at the  $K$  point. We present *ab initio* calculations which agree very well with the experiment. The minimum of the transverse branch at the  $K$  point is due to a strong electron-phonon coupling for this phonon. This coupling dominates the scattering mechanism in both electronic transport and Raman scattering.

Many properties of carbon nanotubes are closely related to those of graphite. The simplest approximation is the zone-folding approach, where the Brillouin zone of a graphite sheet (graphene) is cut into lines that correspond to the allowed states of the nanotube. For the phonon spectrum of nanotubes, there are some fundamental limitations to this approximation, such as the presence of four acoustic modes in one-dimensional systems like nanotubes, and the finite  $\Gamma$ -point frequency of the radial breathing mode, which corresponds to an acoustic mode in graphene. Nevertheless, since it has not been possible to measure the phonon dispersion of carbon nanotubes directly, we need to understand the vibrational properties of graphite very well. Surprisingly, the in-plane graphite phonon dispersion has not been reported completely from experiments. Only the acoustic branches below  $\approx 400 \text{ cm}^{-1}$  were measured by inelastic neutron scattering [1]. The optical phonons between the  $\Gamma$  and  $K$  point and between the  $\Gamma$  and  $M$  point were covered by electron-energy loss spectroscopy [2, 3, 4], but experimental data are missing near the zone boundaries and in the third high-symmetry direction  $K$ - $M$ .

In this paper we present the optical phonon branches in the entire in-plane graphite Brillouin zone determined by inelastic X-ray scattering [5]. Our results show that in particular around the  $K$  point the phonon dispersion was incorrectly predicted by force-constants as well as by *ab initio* calculations [6, 7, 8]. The branch of the transverse optical phonon (TO) is strongly softened at the  $K$  point, suggesting a large coupling to the electronic system. Our *ab initio* calculations agree very well with the experimental data if the long-range nature of the forces in a semimetal like graphite is included. We discuss the implications of the softened  $K$ -point phonons for graphite and carbon nanotubes with respect to electron-phonon coupling and the disorder-induced Raman spectrum.

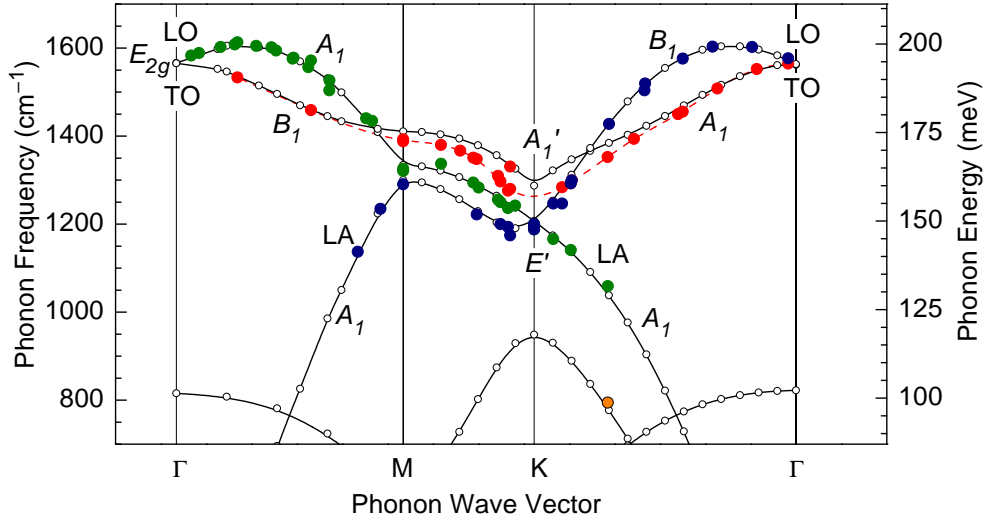


**FIGURE 1.** Phonon dispersion of graphite from inelastic X-ray scattering along the in-plane high-symmetry directions (full circles). The dashed line is a cubic-spline interpolation to the TO-derived branch. The open circles show an *ab initio* calculation for graphene, downscaled by 1%.

Inelastic X-ray measurements were performed at beamline ID28 at the European Synchrotron Radiation Facility. We used an incident beam of 17794 eV focused to a spot size of  $30 \times 60 \mu\text{m}^2$ . The energy resolution was 3.1 meV. The sample was a naturally grown graphite flake consisting of microcrystals with  $\approx 100 \times 200 \mu\text{m}^2$  size.

In Fig. 1 the experimentally obtained phonon dispersion is shown along the  $\Gamma$ -M,  $\Gamma$ -K and  $K$ -M directions (full circles). The bands are labeled by their symmetry and by their displacements at the  $\Gamma$  point, LO (longitudinal optical), LA (longitudinal acoustic), and TO. We will use these labels for the entire branches, although the phonons are strictly transverse or longitudinal only at the  $\Gamma$  point and along  $\Gamma$ -M. The measured frequencies close to the  $\Gamma$  point agree with the  $\Gamma$ -point frequency known from Raman scattering. In the longitudinal optical branch, an overbending of  $\approx 30 \text{ cm}^{-1}$  is clearly seen. The TO and LO bands cross between the  $\Gamma$  and M point and between the  $\Gamma$  and K point. The greatest difference of the experimental data to many of the theoretical predictions is the shape of the TO branch near the K point. It has a minimum at the K point, invalidating force-constants calculations that predicted a local maximum [6], and its frequency is much closer to the LO/LA frequency than predicted from previous *ab initio* calculations [7, 8].

The open circles in Fig. 1 are an *ab initio* calculation within density-functional theory in the generalized gradient approximation, using the SIESTA package [9, 10]. The phonon dispersion is calculated in a supercell approach. Therefore in a semimetal with long-ranged forces, the calculated phonon frequencies are correct only at wave vectors commensurate with the chosen supercell. The agreement of our calculations with the experiment in Fig. 1 is very good; the softening at the K point is still a little underestimated for the TO branch. To obtain the good agreement, it was necessary to explicitly include the K point by taking an appropriate supercell (consisting of multiples of three of the unit cell). This indicates a strong electron-phonon coupling of the TO-

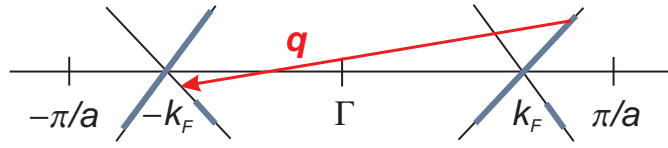


**FIGURE 2.** Schematic view of the linear electronic bands in an armchair tube. They cross at  $k_F = 2/3\pi/a$  ( $a$  is the lattice constant of graphite), which corresponds to the graphite  $K$  point. A fully symmetric phonon with  $q \approx 2k_F \equiv k_F$  can scatter the electrons near the Fermi level.

derived  $K$ -point phonon ( $A'_1$  symmetry) with the electronic system, which is missed in calculations that do not include the  $K$  point. We calculated the electronic density of states in equilibrium and for atomic coordinates that were displaced according to the  $A'_1$  phonon at the  $K$  point. In the case of the displaced atoms, a gap opens at the Fermi level, supporting the large electron-phonon coupling.

The  $K$  point in graphite and the  $K$ -point derived states in carbon nanotubes are special points in the Brillouin zone. At the  $K$  point, the conduction and valence bands cross at the Fermi level in a graphite sheet. A wave vector  $q$  connecting two equivalent  $K$  points is a reciprocal lattice vector, *i.e.*,  $q = 0$ ; a vector connecting two non-equivalent  $K$  points is a  $K$ -point vector itself ( $q = K$ ). Thus to couple electrons near the Fermi level, a  $B_1$ -symmetry phonon with  $q \approx 0$  or a fully symmetric one with  $q \approx K$  is required. The latter is given by the TO-derived mode ( $A'_1$ ) at the  $K$  point. An analogous scattering process takes place in metallic carbon nanotubes. In Fig. 2 we show backscattering of electrons by this phonon in electronic transport. Transport measurements in carbon nanotubes indicate that indeed scattering by the phonons corresponding to the  $K$ -point TO in graphite dominates the backscattering mechanism [11, 12]. In these experiments, the current saturates after the electrons have gained an energy of about 160 meV, which is close to the energy of the TO phonon at the  $K$  point.

Similarly to the backscattering shown in Fig. 2, the excited electrons are scattered in the double-resonant Raman process that gives rise to the  $D$  mode in both graphite and carbon nanotubes [13, 14, 15]. Again, the  $D$  mode is constituted by the fully symmetric TO-phonons from near the  $K$  point [16]. We confirm this explicitly by calculating the  $D$  mode of graphite in the linear approximation [17], using the experimental phonon dispersion. In Fig. 3 we show the  $D$ -mode frequency as a function of excitation energy from a calculation with the TO branch (solid lines) and with the LO branch (dashed lines). It is clearly seen that the results of the TO branch agree very well with the experimental data (solid circles), whereas the LO-based calculations do not reproduce the experiments.

Finally, we want to illustrate what we expect for carbon nanotubes. In Fig. 4 we show the phonon dispersion of the  $m = 0$  and  $m = n$  bands in armchair and zig-zag tubes, obtained from the experimental data in Fig. 1 by zone folding. As mentioned above, zone folding contains systematic errors for the phonon dispersion; for example, the nanotube  $\Gamma$ -point

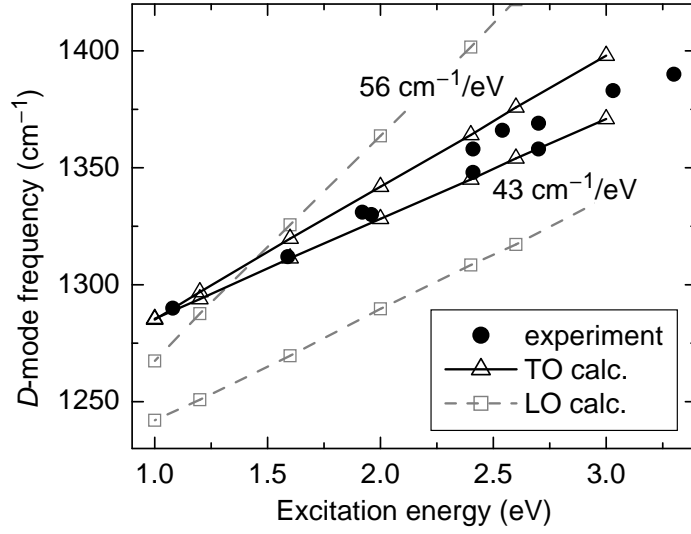


**FIGURE 3.** *D*-mode frequency in graphite as a function of laser energy calculated within the double-resonance model in the linear approximation. The triangles/solid lines (squares/dashed lines) were calculated using the TO (LO)-derived phonon branch. The calculation from the TO-derived branch matches the experimental values (full circles) very well. Experimental values are taken from Refs. [18, 19, 20].

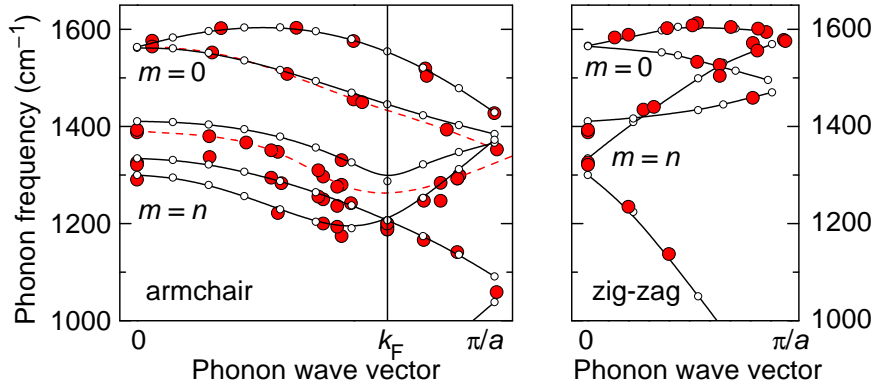


**FIGURE 4.** Zone-folding of the graphite dispersion; the symbols are the same as in Fig. 1. The folded branches of graphite form the  $m = 0$  and  $m = n$  branches in zig-zag tubes ( $\Gamma$ - $M$ ) and in armchair tubes ( $\Gamma$ - $K$ - $M$  direction).

modes should be split, and the  $m = 0$  and  $m = n$  bands should depend on the diameter. Nevertheless, we see that the graphite  $K$  point is transformed into the Fermi wave vector in metallic carbon nanotubes. As shown in Fig. 2, electrons at  $k_F$  and at  $-k_F$  are coupled by phonons with  $q = k_F$ . Therefore, we predict a similar softening of the fully symmetric phonon band at  $k_F$  in carbon nanotubes as we observed in graphite.

In summary, we determined the phonon dispersion of graphite by inelastic X-ray scattering. The experimental results invalidate some of the existing theories, in particular,

we found near the  $K$  point a much stronger dispersion of the TO-derived, fully symmetric branch than predicted. We presented *ab initio* calculations, which agree very well with the experiment. The softening of the  $A'_1$  mode at the  $K$  point is caused by a strong electron-phonon coupling, which is predicted for carbon nanotubes as well. This coupling leads to the double-resonant  $D$  mode in the Raman spectra of graphite and carbon nanotubes. We calculated the  $D$  mode using the experimental phonon dispersion and confirmed the symmetry-based prediction that the  $D$  mode comes from the TO-derived branch.

## ACKNOWLEDGMENTS

We acknowledge support from the Deutsche Forschungsgemeinschaft under grant number Th 662/8-2 and from the ESRF. S.R. was supported by the Oppenheimer Fund and Newnham College. P.O. was supported by Spain's MCyT project BFM2003-03372-C03. We also acknowledge support from the Ministerio de Ciencia y Tecnología (Spain) and the DAAD (Germany) for a Spanish-German Research action (HA2001-0065).

## REFERENCES

1. Nicklow, R., Wakabayashi, N., and Smith, H. G., *Phys. Rev. B*, **5**, 4951 (1972).
2. Wilkes, J. L., Palmer, R. E., and Willis, R. F., *J. Electron Spectr. Rel. Phen.*, **44**, 355 (1987).
3. Oshima, C., Aizawa, T., Souda, R., Ishizawa, Y., and Sumiyoshi, Y., *Solid State Comm.*, **65**, 1601 (1988).
4. Siebentritt, S., Pues, R., and Rieder, K.-H., *Phys. Rev. B*, **55**, 7927 (1997).
5. Maultzsch, J., Reich, S., Thomsen, C., Requierdt, H., and Ordejón, P., *Phys. Rev. Lett.*, **92**, 075501 (2004).
6. Jishi, R. A., and Dresselhaus, G., *Phys. Rev. B*, **26**, 4514 (1982).
7. Sánchez-Portal, D., Artacho, E., Soler, J. M., Rubio, A., and Ordejón, P., *Phys. Rev. B*, **59**, 12678 (1999).
8. Dubay, O., and Kresse, G., *Phys. Rev. B*, **67**, 035401 (2003).
9. Junquera, J., Paz, O., Sánchez-Portal, D., and Artacho, E., *Phys. Rev. B*, **64**, 235111 (2001).
10. Soler, J. M., Artacho, E., Gale, J. D., García, A., Junquera, J., Ordejón, P., and Sánchez-Portal, D., *J. Phys.: Cond. Mat.*, **14**, 2745 (2002).
11. Yao, Z., Kane, C. L., and Dekker, C., *Phys. Rev. Lett.*, **84**, 2941 (2000).
12. Bourlon, B., Glattli, D., Plaçais, B., Berroir, J., Miko, C., Forró, L., and Bachtold, A., *Phys. Rev. Lett.*, **92**, 026804 (2004).
13. Thomsen, C., and Reich, S., *Phys. Rev. Lett.*, **85**, 5214 (2000).
14. Maultzsch, J., Reich, S., and Thomsen, C., *Phys. Rev. B*, **64**, 121407(R) (2001).
15. Reich, S., Thomsen, C., and Maultzsch, J., *Carbon Nanotubes: Basic Concepts and Physical Properties*, Wiley-VCH, Berlin, 2004.
16. Mapelli, C., Castiglioni, C., Zerbi, G., and Müllen, K., *Phys. Rev. B*, **60**, 12710 (1999).
17. Maultzsch, J., Reich, S., and Thomsen, C. (2004), to be published.
18. Wang, Y., Alsmeyer, D. C., and McCreery, R. L., *Chem. Mater.*, **2**, 557 (1990).
19. Pócsik, I., Hundhausen, M., Koos, M., and Ley, L., *J. Non-Cryst. Sol.*, **227-230B**, 1083 (1998).
20. Matthews, M. J., Pimenta, M. A., Dresselhaus, G., Dresselhaus, M. S., and Endo, M., *Phys. Rev. B*, **59**, R6585 (1999).